Programmable agile beam steering based on a liquid crystal prism*

Xu Lin(徐 林)†, Huang Zi-Qiang(黄子强), and Yang Ruo-Fu(杨若夫)

School of Optoelectronic Information, University of Electronic Science and Technology of China, Chengdu 610054, *China*

(Received 2 April 2011; revised manuscript received 23 May 2011)

To meet the application need for agile precision beam steering, a novel liquid crystal prism device with a simple structure, convenient control, low cost and applicable performance is presented, and analysed theoretically and experimentally. The relationships between the optical path and the thickness of the liquid crystal cell under different voltages are investigated quantitatively by using a theoretical model. Analysis results show that the optical path profile of the liquid crystal prism has a quasi-linear slope and the standard deviation of the linear slope is less than 16 nm. The slope ratio can be changed by a voltage, which achieves the programmable beam steering and control. Practical liquid crystal prism devices are fabricated. Their deflection angles and wavefront profiles with different voltages are experimentally tested. The results are in good agreement with the simulated results. The results imply that the agile beam steering in a scope of 100 μrad with a micro-rad resolution is substantiated in the device. The two-dimensional beam steering is also achieved by cascading two liquid crystal prism devices.

Keywords: liquid crystal, polarization devices, beam steering, optical scanner

PACS: 42.70.Df **DOI:** 10.1088/1674-1056/20/11/114216

1. Introduction

Agile beam steering technology is critical for many applications, such as free space optical communication, optical interconnection and lidar. Compared with traditional mechanical type devices, non-mechanical beam steering ones are attracting attention due to their small size, light weight and low power consumption. Recently, the non-mechanical beam steering approaches mainly include lenslet arrays, micro-electro-mechanical systems (MEMs), electrowetting and liquid crystal optical phased arrays.[1−7] However, devices based on those approaches are expensive and difficult to manufacture, which restrains their applications to some extent.

The liquid crystal (LC) prism can be used in a simple and applicable alternative approach. According to the electrode pattern, the LC prisms can be divided into two types: stair-case and continuous-ramp phase modulations. The former uses discrete electrodes, while the latter uses uniform electrodes and is easier to manufacture and control. The LC prism with continuous phase modulation can be implemented with different methods. For example, Gordon *et al.*,[8] Andrii *et al.*,[9] Nabeel and Sajjad,[10] and Sajjad and Nabeel[11] separately achieved the ramp-like optical path profile by producing a voltage ramp across the LC cell using the resistance effect of the electrode. While Jae and Iam[12] achieved the profile by forming a polymer wedge in the LC cell. The same feature of those devices is that the thicknesses of the LC cells are all uniform. In the present paper, we present a novel LC prism with a simple structure, convenient control, low cost and applicable performance. The manufacture technique process of this LC prism is nearly the same as that of an ordinary LC cell. The only difference is in the control condition of the cell thickness. The details are described in the following.

2. Structure and principle of LC prism

The basic structure of the proposed LC prism is a wedge-shape LC cell as shown in Fig.1. The cell consists of two indium tin oxide (ITO) glass substrates, between which is a wedge-like layer of nematic liquid crystal material. The wedge-like layer is controlled by two sphere spacers with different diameters, which are sprinkled individually on two opposite sides of the LC

*Project supported by the National High Technology Research and Development Program of China (Grant No. 2009AA8042017) and the Postdoctoral Science Foundation of University of Electronic Science and Technology of China.

†Corresponding author. E-mail: hitlinzexu@163.com

© 2011 Chinese Physical Society and IOP Publishing Ltd

cell. The diameters of the two sphere spacers are D_1 and D_2, with $D_1 \neq D_2$. Due to the difference between D_1 and D_2, a wedge-like optical path or phase profile will occur when a plane optical wave incidences at the cell.

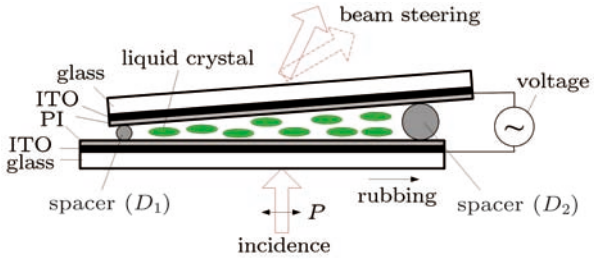


Fig. 1. (colour online) Basic structure of the LC prism.

The inner surfaces of the two ITO glass substrates are coated with polyimide (PI) films. The PI film is rub treated, thereby producing an anchor effect that makes the liquid crystal molecules align along the rubbing direction. The rubbing directions of the two substrates are identical. So the liquid crystal molecules in the cell are in parallel alignment, and the alignment direction is kept parallel or perpendicular to the slope direction of the wedge. Due to the wedge-like liquid crystal layer, a slope profile of optical path across the LC cell is produced, which will induces the beam deflection with an initial bias angle. In addition, the slope ratio will vary slightly when different voltages are applied to the two ITO electrodes of the LC cell. This implies that the deflection angle can be precisely changed from the initial bias angle. Since the driving voltage can be conveniently controlled by using programmable modules, a programmable agile beam steering can be achieved by using the liquid crystal prism proposed in this paper.

3. Simulation analysis

The characteristic of the liquid crystal prism is that the thickness of the liquid crystal layer has a slope profile. To simplify the problem, firstly we set up a one-dimensional model of an ordinary liquid crystal cell to simulate the liquid crystal director profile in the LC cell under an electric field and analyse the influence of the variation of the cell thickness. The basic structure of an ordinary LC cell consists of seven layers, as shown in Fig. 2. According to the Frank–Oseen continuum theory, the Gibbs free energy density in the LC cell can be described as[13]

$$f_{\mathrm{G}} = \frac{1}{2}K_{11}(\nabla \cdot \boldsymbol{n})^2 + \frac{1}{2}K_{22}(\boldsymbol{n} \cdot \nabla \times \boldsymbol{n})^2 + \frac{1}{2}K_{33}(\boldsymbol{n} \times \nabla \times \boldsymbol{n})^2 - \frac{1}{2}\boldsymbol{D} \cdot \boldsymbol{E}, \quad (1)$$

where $\boldsymbol{n} = (n_x, n_y, n_z)$ is the LC director; K_{11}, K_{22}, and K_{33} are the splay, the twist, and the bend constants, respectively; $\boldsymbol{D} = \boldsymbol{\varepsilon}\boldsymbol{E}$ and $\boldsymbol{E} = -\nabla\varphi$ are the electric displacement and the electric field intensity, respectively, with φ being the potential and $\boldsymbol{\varepsilon}$ being the dielectric tensor of the liquid crystal material. Under the one-dimensional condition, $n_{\mathrm{y}} = 0$ and $\partial/\partial x = 0$, then the whole Gibbs free energy G in the LC cell is

$$G = \int f_{\mathrm{G}}(n_x, n_z, \partial n_x/\partial z, \partial n_z/\partial z, \partial\varphi/\partial z)\,\mathrm{d}\tau. \quad (2)$$

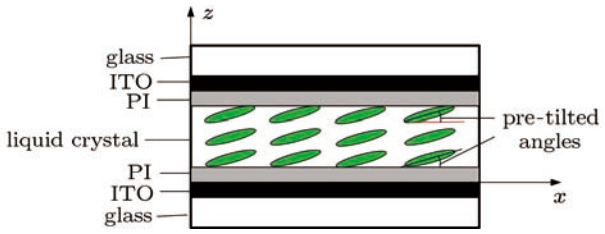


Fig. 2. (colour online) Structure model of ordinary liquid crystal cell.

The Gibbs free energy G will attain its minimum when the liquid crystal molecules are in equilibrium. Calculate the variation of the Gibbs free energy density and let the variation equal zero, then the Euler–Lagrange equations with respect to director n_i and potential φ will be derived as

$$[f_{\mathrm{G}}]_{\varphi} = \frac{\partial f_{\mathrm{G}}}{\partial\varphi} - \sum_{j=x,y,z}\frac{\mathrm{d}}{\mathrm{d}j}\left[\partial f_{\mathrm{G}}/\partial\left(\frac{\mathrm{d}\varphi}{\mathrm{d}j}\right)\right] = 0, \quad (3)$$

$$[f_{\mathrm{G}}]_{n_x} = \frac{\partial f_{\mathrm{G}}}{\partial n_x} - \sum_{j=x,y,z}\frac{\mathrm{d}}{\mathrm{d}j}\left[\partial f_{\mathrm{G}}/\partial\left(\frac{\mathrm{d}n_x}{\mathrm{d}j}\right)\right] = 0, \quad (4)$$

$$[f_{\mathrm{G}}]_{n_z} = \frac{\partial f_{\mathrm{G}}}{\partial n_z} - \sum_{j=x,y,z}\frac{\mathrm{d}}{\mathrm{d}j}\left[\partial f_{\mathrm{G}}/\partial\left(\frac{\mathrm{d}n_z}{\mathrm{d}j}\right)\right] = 0. \quad (5)$$

We calculate the Euler–Lagrange equations by using the hybrid difference iterative algorithm, which is based on the Double–Sweep Method.[14] The liquid crystal material parameters are assumed to be $K_{11} = 11.1 \times 10^{-12}$ N, $K_{33} = 17.1 \times 10^{-12}$ N, $\varepsilon_{\parallel} = 19.0$, $\varepsilon_{\perp} = 5.2$, $n_{\mathrm{o}} = 1.521$, and $n_{\mathrm{e}} = 1.7461$, where o and e stand for ordinary and extraordinary, respectively. Other parameters used are dielectric constant $\varepsilon_{\mathrm{PI}} = 3.0$, pre-tilted angle 2°, PI layer thickness 0.1 μm, and wavelength 632.8 nm. The calculated voltage-director profiles (tilted angle θ_z) with different cell thicknesses are shown in Fig. 3, where the upturned arrows represent the cell thickness increasing from down to up, i.e. 5 μm, 8 μm, and 11 μm

in order. It can be seen that the LC director profile varies with the cell thickness.

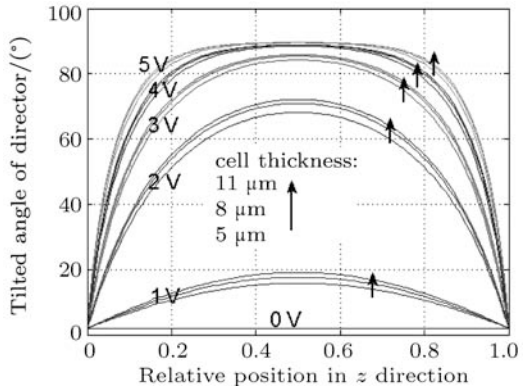


Fig. 3. Calculated voltage-director profiles with different cell thicknesses.

Based on the optical characteristic, the liquid crystal is considered as a mono-axial crystal. The effective refractive index $n_{\rm eff}$ of the LC cell can be attained from the calculated director profile as

$$n_{\rm eff} = \frac{1}{L}\int_0^L n_{\rm e}(z)\,{\rm d}z, \tag{6}$$

where L is the cell thickness, and $n_{\rm e}(z)$ is the distributional refractive index for the extraordinary light in the liquid crystal cell and is expressed as

$$n_{\rm e}(\theta_z) = \frac{n_{\rm e}n_{\rm e}}{\sqrt{n_{\rm o}^2\cos^2\theta_z + n_{\rm e}^2\sin^2\theta_z}}. \tag{7}$$

Then the optical path (OP) through the liquid crystal layer is

$$L_{\rm OP} = n_{\rm eff}L = \int_0^L n_{\rm e}(z)\,{\rm d}z. \tag{8}$$

Here, it is noted that the optical path or the phase is for the extraordinary light unless otherwise indicated in this paper. In order to analyse the effects of cell thickness and voltage together on the optical path, both the cell thickness and the voltage are changed simultaneously. The characteristic profiles of the optical path with different cell thicknesses and voltages are shown in Fig. 4.

Specially, we give the relationships between the cell thickness and the optical path with different voltages, which are shown in Fig. 5. It can be seen that for a given voltage, the increase of the optical path is proportional to the increase of the cell thickness. In order to evaluate the linearity of the relationship, we fit each of the cell thickness–optical path curves with different voltages by a linear function. The maximum standard deviation is less than 16 nm, which is about one thousandth of the optical path. Therefore the relationship between the optical path and the cell thickness can be accurately described by a linear function. It is also found that slope ratio k of the optical path fitting line varies with the voltage. These two characteristics are completely similar to those of a prism, whose wedge angle is variable by the control voltage. So the liquid crystal can be used to achieve the programmable beam steering.

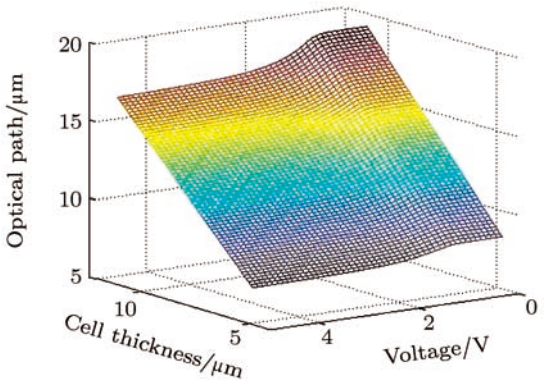


Fig. 4. (colour online) Optical path versus cell thickness and voltage.

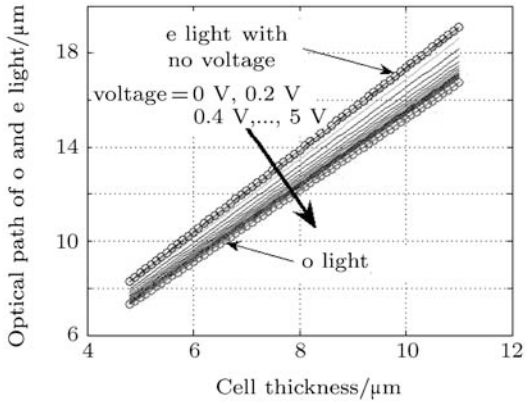


Fig. 5. Optical path of the LC cell versus cell thickness.

Based on the two above characteristics of the liquid crystal, we conceive the wedge-shape LC cell device described in Section 2. Then the two characteristics, i.e. the increase of the optical path is proportional to the increase of the cell thickness and slope ratio k of the optical path fitting line varies with the voltage, can be used in this wedge-shaped LC cell.

We assume that the diameters of the two spacers are $D_1 = 6$ μm and $D_2 = 11$ μm, and that the distance between the two spacers is $d = 11$ mm, then the beam deflection angle θ can be calculated by

$$\theta = \arctan((k-1)\,|D_1 - D_2|\,/d), \tag{9}$$

where $(k-1)\cdot|D_1-D_2|$ denotes the whole optical path including the additional optical path produced by the

air wedge outside the LC cell. The calculated relationship curve between deflection angle θ and the voltage is shown in Fig. 6. It can be seen that the deflection angle has a bias value of approximately 340 μrad corresponding to the voltage of 0 V. When a programmable voltage is applied, the beam steering and scanning in a scope from about 240 μrad to 340 μrad can be achieved.

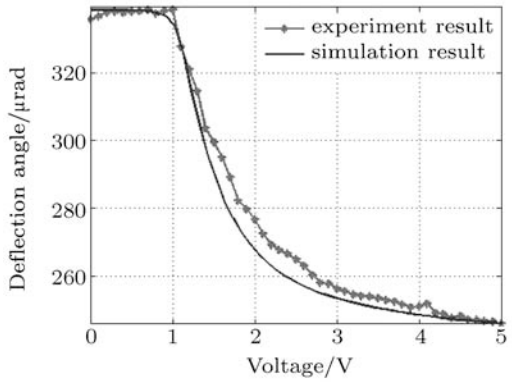


Fig. 6. Beam deflection angle versus driving voltage.

4. Experiments

4.1. One-dimensional beam steering

According to the structure described in Section 2, we fabricate an LC prism device with an aperture of 15 mm×15 mm. The liquid crystal material is E7 from the Merck Company. The diameters of the two spacers are $D_1 = 6$ μm and $D_2 = 11$ μm. The distance between the two spacers is 11 mm. When a programmable altering current (AC) voltage is applied across the two ITO electrodes, the programmable beam steering is achieved. We set up an optical platform, which is shown in Fig. 7, to test the beam steering characteristic and the sketch of the experimental principle.

A He–Ne laser beam with the wavelength of 632.8 nm passes through the circle aperture, the attenuator, and the polarizer in sequence, and then impinges on the LC prism. Here, the transmission axis of the polarizer is parallel to the rubbing direction of the LC cell. The output deflection beam continues to pass through a lens and impinges as a light spot on a CCD array, which is located at the focus plane of the lens. According to the location variation of the spot in the CCD, deflection angle θ of the output beam can be deduced from formula $\theta = \arctan(\Delta x/f)$, where $f = 500$ mm is the focus length of the lens, and Δx is the location variation in the x orientation relative to the initial spot location obtained on the condition that the LC prism is not inserted into the light path. Since the actual light spot has a small size, the spot location is calculated by using the centre-of-gravity method. We use a signal generator to produce a 1 kHz sinusoid voltage to drive the LC prism. By changing the root-mean-square (RMS) value of the sinusoid voltage, a series of deflection spots are captured by the CCD. Therewith, the measured deflection angles with different voltages are obtained and are shown in Fig. 6. It can be seen that the measured deflection angles are in good agreement with the simulation results, showing that the theoretical model and the analysis are considerably accurate. Although the beam deflection scope is not large, the angle resolution is at least better than 1 μrad. Theoretically, the deflection angle resolution depends on the resolution of the driving voltage. In our experiment, the voltage resolution of the signal generator is only 0.1 Vrms. If it is improved to 10 mVrms, the angle resolution can be improved to be better than 100 nrad. In addition, an interesting phenomenon is that the voltage–deflection angle curve of the LC prism is completely similar to the voltage–optical path curve of the liquid crystal material, which may be due to the linear relationship between the optical path and the cell thickness in the LC prism at any voltage.

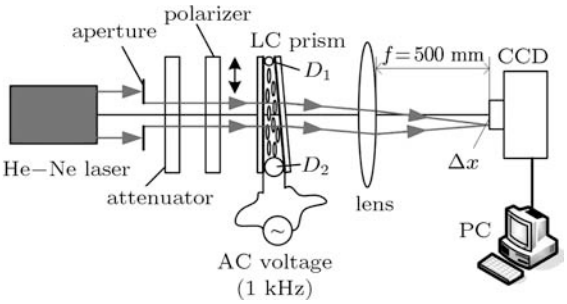


Fig. 7. Measurement set up of beam deflection experiment.

4.2. Two-dimensional beam steering

A single LC prism can achieve the one-dimensional beam steering and scanning. Now we cascade two LC prisms together, whose slope gradient directions are perpendicular to each other and the rubbing directions are parallel to each other. Applying two driving voltages to the two LC prisms separately, then beam steerings in the x and the y directions are independent. Employing the measurement set up in Fig. 7, we acquire the experiment results shown in Fig. 8. For the convenience of expression, two curves

of voltage–deflection angles in the x and the y directions are plotted in the same figure. The results show

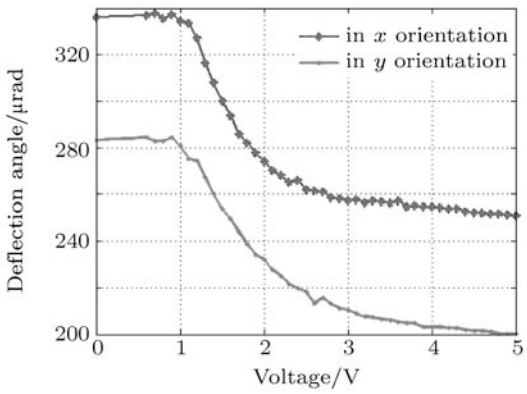


Fig. 8. Measurement results of two-dimensional beam steering experiment.

that the two-dimensional beam steering is completely feasible by means of cascading two LC prisms, although the deflection angle biases of the two curves are different due to the difference in the distance between the two spacers in the two LC prisms.

4.3. Wavefront profile measurement of deflection beam

To test the quality of the deflection beam, we set up a Mach–Zehnder phase shift interferometer[15] to measure the wavefront profile of the output beam deflected by the LC prism. Measurement results are shown in Fig. 9, where figure 9(a) shows the initial wavefront with the voltage of 0 V and figures 9(b)–9(f) show wavefronts relative to their initial ones corresponding to the voltages of 1–5 V, respectively. It can be seen that the wavefront from the LC prism is considerably flat. The standard deviation of the wavefront distortion is less than 0.4λ, which indicates that the wavefront distortion produced from the LC prism is very gentle. If we use more flat ITO glasses, the distortion can be reduced further.

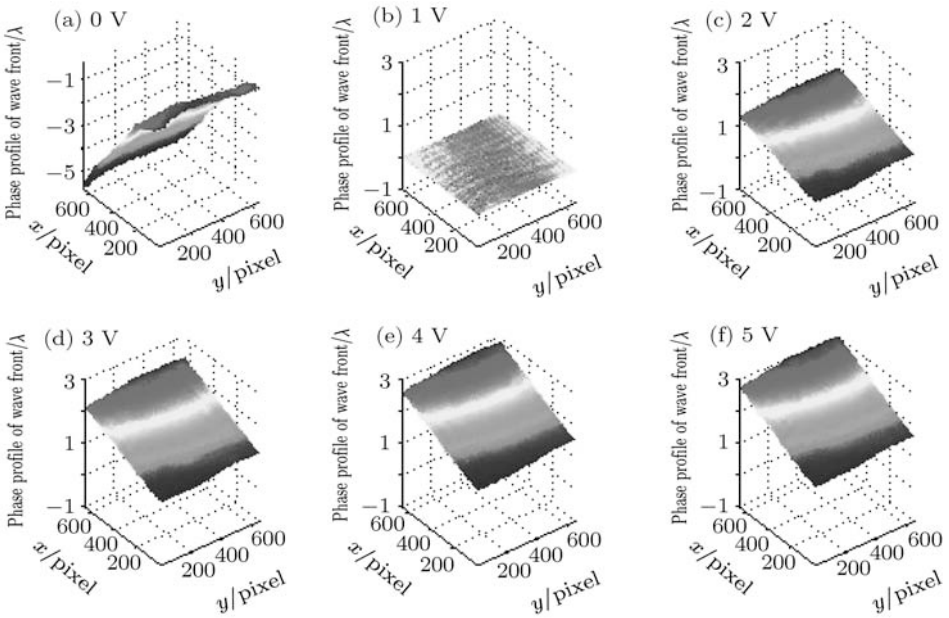


Fig. 9. Measurement results of wavefront profiles from LC prism: (a) initial wavefront with voltage of 0 V; (b)–(f) wavefronts relative to their initial one corresponding to voltages of 1–5 V, respectively.

5. Conclusion

A novel LC prism device with a simple structure, convenient control, low cost and applicable performance is presented and analysed for agile beam steering applications. A one-dimensional model of the LC prism is set up to analyse the effects of cell thickness and voltage on the optical path. It is shown that the increase of the optical path is nearly proportional to the increase of the cell thickness and slope ratio k of the optical path fitting line varies with the increase of the voltage. Based on these two characteristics, the relationship between the beam deflection angle and the voltage is deduced theoretically. We fabricate LC prism devices practically and perform a one-dimensional beam steering experiment. The experimental results are in good agreement with the theoretical results. In addition, the two-dimensional beam

steering is achieved by cascading two LC prism devices. The beam wavefront from the LC prism is also tested by using a Mach–Zehnder phase shift interferometer. The results show that the agile beam steering is completely feasible and applicable.

References

[1] Paul F M, Philip J B, Michael J E, Jason H, Steve S, Xie H K and Edward A W 2009 *Proc. IEEE* **97** 1078

[2] Liu X, Zhang J, Wu L Y and Gan Y 2011 *Chin. Phys.* B **20** 024211

[3] Liu C, Mu Q Q, Hu L F, Cao Z L and Xuan L 2010 *Chin. Phys.* B **19** 064212

[4] Zhang J, Fang Y, Wu L Y and Xu L 2010 *Chin. J. Las.* **37** 325 (in Chinese)

[5] Cai D M, Ling N and Jiang W H 2008 *Acta Phys. Sin.* **57** 897 (in Chinese)

[6] Zheng J H, Zhong Y W, Wen K, Luo X S and Zhuang S L 2010 *Acta Phys. Sin.* **59** 1831 (in Chinese)

[7] Yu Y J, Wang T and Zheng H D 2009 *Acta Phys. Sin.* **58** 3154 (in Chinese)

[8] Gordon D L, John V M and Alan P 1994 *Opt. Lett.* **19** 1170

[9] Andrii B G, Sergij V S and Oleg D L 2005 *Proceeding of SPIE–Emerging Liquid Crystal Technologies*, January 25–27, 2005 San Jose, United States, p. 146

[10] Nabeel A R and Sajjad A K 2003 *Opt. Lett.* **28** 561

[11] Sajjad A K and Nabeel A R 2004 *Opt. Express* **12** 868

[12] Jae H P and Iam C K 2005 *Appl. Phys. Lett.* **87** 091110

[13] de Gennes P G and Prost J 2008 *The Physics of Liquid Crystals* (2nd edn.) (Beijing: Science Press) p. 8

[14] Xu L, Zhang J and Wu L Y 2007 *Infra. Las. Eng.* **36** 932 (in Chinese)

[15] Friedman L J, Hobbs D S, Lieberman S and Corkum D L 1996 *Appl. Opt.* **35** 6236